DUPLEX S-N CURVE CHARACTERISTICS AND SUBSURFACE FATIGUE CRACK INITIATION BEHAVIOUR IN HIGH CARBON-CHROMIUM BEARING STEEL

K. Shiozawa, L. T. Lu, and S. Ishihara,
Department of Mechanical Systems Engineering, Toyama University,
3190 Gofuku, Toyama 930-8555, JAPAN

ABSTRACT

The S-N curve obtained from cantilever-type rotary bending fatigue tests using hourglass shaped specimens of high carbon-chromium bearing steel was clearly classified fracture modes into two groups of different crack origin. One was governed by a crystal slip on the specimen surface, which occurred in the region of short fatigue life and high stress amplitude level. The other was governed by nonmetallic inclusion at subsurface which occurred in the region of long fatigue life and low stress amplitude. The inclusion governed fish-eye fracture mode was distributed in a wide range of stress amplitude not only below the fatigue limit defined as the threshold of fracture due to the slip governed mode but also above the fatigue limit. This remarkable shape of the S-N curve was different from a step-wise one reported in previous literature and was characterized as duplex S-N curves which composed of two different S-N curves corresponding to the respective fracture modes. From the detailed observation of fracture surface and fatigue crack origin, mechanisms of internal fracture mode and characteristics of S-N curve were discussed.

INTRODUCTION

It is well known that a S-N curve of iron and low-carbon steel obtained from fatigue test in air usually turns to horizon in neighborhood of the 10^6-10^7 cycles and show clear fatigue limit which is used for fatigue design of machine components and structures as a standard. In recent year, an attention has been attracted on fatigue behavior of materials in high cycle region, that is ultra-long life region (>10^7 cycles), because of requirement for high efficiency and reliability to the machines and structures, and increase in aging facilities exceeding 10^8 cycles [1-4]. Although a large amount of fatigue data has been reported in the form of S-N curves, the data in literature have been unfortunately limited to fatigue lives up to 10^7 cycles. Generally speaking, ordinary fatigue crack initiation occur mostly on the specimen surface owing to slip deformation. However, fatigue failure is occurred at small internal defect on the subsurface of a material, especially a high-strength steel and a case-hardened steel [5]. Subsurface crack initiation was dominant at the region of low stress amplitude and high cycling, while the surface fatigue crack initiation occurred at the region of high stress amplitude and low cycling. It is revealed that there is a definite stress range where the crack

initiation site changes from the surface to the subsurface defect, known as a step-wise S-N curve, that is, there are two knees on the curve. It is an interesting practical problem for design why fracture mode transition from surface to the interior occurs in long fatigue life range. There is little information about the mechanisms of subsurface crack initiation and propagation.

The aim of this study is to clarify the complicated fatigue behavior of structural materials in long life region. In this investigation, the experimental data in the gigacycle fatigue range were obtained through a cantilever-type rotating-bending fatigue test in air using the specimen of high carbon-chromium bearing steel. According to the quantitative analysis of the fractography of the fracture surface, subsurface crack initiation behavior and the characteristics of S-N curve were discussed.

EXPERIMENTAL PROCEDURES

Testing Material and Specimen

The material used in this study was high carbon-chromium bearing steel, JIS SUJ2. The chemical composition (mass %) of this steel is 1.01 C, 0.23 Si, 0.36 Mn, 1.45 Cr, 0.06 Cu, 0.04Ni, 0.02 Mo, 0.012 P and 0.007 S. Specimens having hourglass-shaped with a minimum diameter of 3 mm and round notch radius of 7 mm were machined from round bar with diameter of 14.3 mm, after that they were quenched for 2.4 ks in a vacuum at 1108 K and oil cooled, and tempered for 1.2 ks in a vacuum at 453 K and air cooled. Round notch surface was polished by a grinder having a mesh of #100 and fatigue tests were performed without any other additional surface treatment. An elastic stress concentration factor of this specimen is 1.06. The Vickers hardness of the specimen heat-treated is HV750±13.4 and uniform from the specimen surface to the inside. Tensile strength of the specimen is 2316 MPa.

Testing Methods

Fatigue tests were performed in an open environment at room temperature using a four-axes cantilever-type rotating-bending fatigue machine which was operated at 3150 rpm (f=52.5 Hz). This multi-type fatigue-testing machine was originally developed by a research group in Japan [4] to perform fatigue tests efficiently, that is, to save the cost and time. The machine has two spindles driven by one electric motor and each spindle has specimen holders at both ends. Therefore, four specimens can be tested simultaneously in cantilever-type rotating bending. A weight applied to specimen is suspended from the outer end of each specimen by means of a bearing and a helical spring.

EXPERIMENTAL RESULTS AND DISCUSSION

S-N Curves

Figure 1 shows the S-N curve obtained from the fatigue tests. Experimental results were separated to two groups as shown in this figure: One group plotted by open circles exists in the range of high stress amplitude from 1700 to 1200 MPa and of short lives. The other plotted by solid circles is in the range of low-stress amplitude from 1500 to 950 MPa and of long lives. These two groups were distinguished by the fatigue crack initiation site, as discuss next section. The former is from surface and the latter is from subsurface of the specimen.

A horizontal solid line to the N_f axis in Figure 1 shows the experimental results of conventional fatigue limit. Estimation of the fatigue limit was conducted by the well-known staircase method using eleven specimens and setting the run-out stress cycles of 10^7. Average

fatigue limit was calculated as 1255 MPa and the standard deviation of 21.8 MPa. After the above tests were finished, every one of run-out specimens was again fatigue tested continuously to rupture.

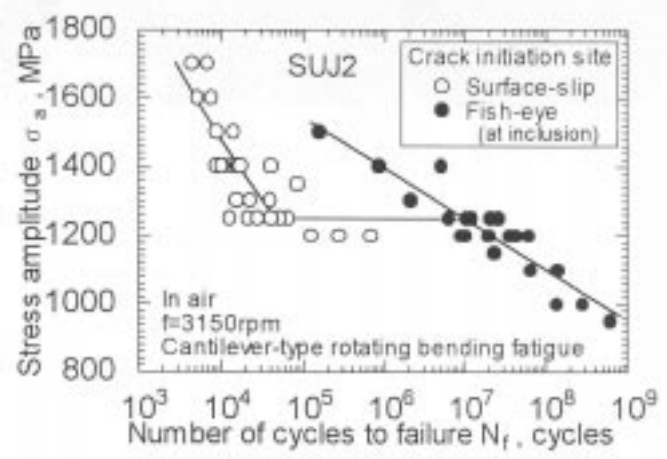

Figure 1: S-N curve of high carbon-chromium bearing steel.

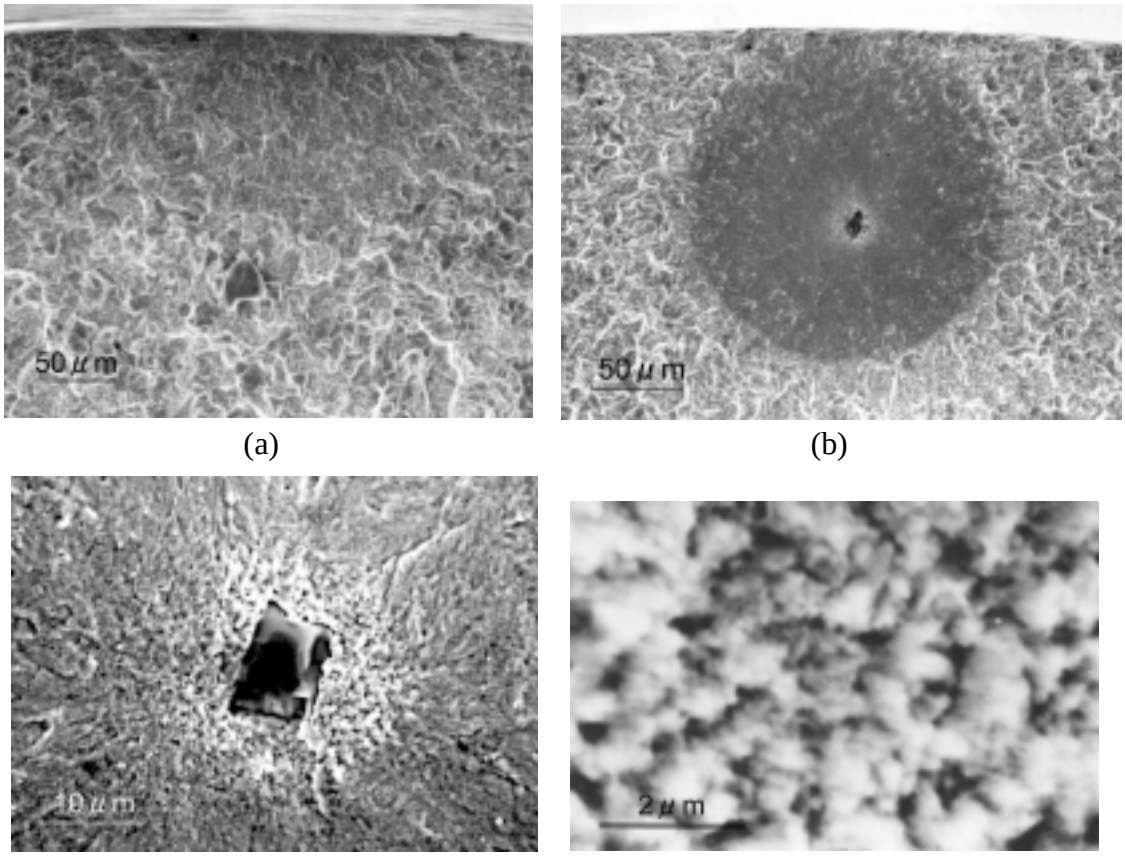

(a) (b)

(c) (d)

Figure 2: Example for SEM observation of surface crack initiation site (a) and fish-eye type fracture surface (c-d).

Fractography

A SEM observation was made for fracture surface of every ruptured specimen. It was seen from observation of the fracture surface that the fatigue crack initiation site was different depending on stress amplitude and number of cycles to failure, and could be classified into two typical modes. One mode was that fatigue crack initiate on specimen surface due to crystal slip. A typical example is shown in Figure 2(a). No significant defect or inclusion was observed at the crack initiation site. The other mode was that fatigue crack initiated from the interior of a specimen, which is called a fish-eye. Figure 2(b) shows an example of a fish-eye

pattern formed on the fracture surface and the nonmetallic inclusion at the center of the fish-eye. The black circular area reveals the trace of fatigue crack growth and the white area is outside of the circular area, which is suggested to form by means of the different crack growth mechanisms. At the center of the fish-eye mark, a bright facet area was found in the vicinity of the inclusion on the fracture origin as shown in Figure 2(c). From the observation of higher magnification, the bright facet area has a quite different fracture surface from the black circular area surrounding it and reveals a very rough and granular morphology [see Fig.2(d)]. The same results were reported recently by Murakami *et al*. [2]. They called the rough morphology at the vicinity of the inclusion a dark area based on the observation by optical microscopy. And also they concluded that the rough morphology may be caused by hydrogen embrittlement coupled with fatigue.

The results classified into two kinds of fracture mode observed by SEM were shown in Figure 1. The experimental plots marked with open circle correspond to fatigue fracture from a surface origin and those marked with solid circle correspond to fracture from internal nonmetallic inclusion having the fish-eye. It can be seen from this figure that the fracture from surface origin occurs at a high stress amplitude level and short life and that from internal inclusion occurs at a low stress amplitude level and long life. The transition of fracture origin from surface to subsurface appears mainly as horizontal step in the S-N curve as shown in Figure 1. But it is interesting that there are some data that show fracture from subsurface inclusion at higher stress amplitude level than the horizontal step in the S-N curve, and two fracture modes reveal at same stress amplitude level according to circumstances. This complex shaped S-N curve obtained in this study is different from the step-wise S-N curve in the literature, that is, there are two knees on the curve.

Figure 3 shows the relationship between rupture probability, P, of the surface crack mode and the subsurface crack mode, and applied stress amplitude. Fatigue tests were performed at three stress amplitude levels of 1400, 1250 and 1200 MPa using 10~14 specimens each stress level and fracture mode was determined by the observation of SEM. It is clearly shown from this figure that both fracture modes reveal in wide stress amplitude level below and upper fatigue limit obtained by the staircase method. The rupture probability of subsurface crack mode increases according to decrease of applied stress amplitude. The same rupture probability of surface crack mode as subsurface one (P=50 %) occurs at a stress level of 1260 MPa, which is the same as the fatigue limit of 1255 MPa.

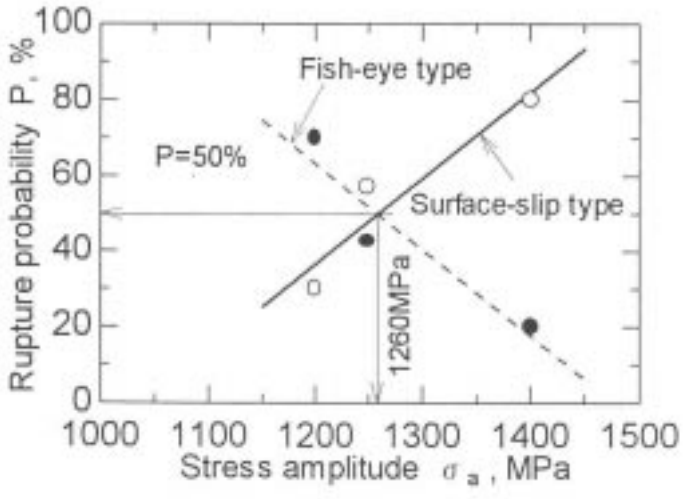

Figure 3: Relationship between rupture probability of surface crack mode and subsurface crack mode, and applied stress amplitude.

Quantitative Evaluation of Crack Initiation Site

Size of Crack Origin

Figure 4 shows experimental relationship between size of crack initiation site, $\sqrt{area}$, and stress amplitude. The area of the crack initiation site was measured from SEM photograph using a computer aided image-processing device. The size of nonmetallic inclusion governed fish-eye fracture mode, $\sqrt{area_{inc}}$, is 6~12 μm and independent to stress amplitude. On the other hand, the size of surface crack initiation site, $\sqrt{area_S}$, which is defined as the size of facet formed by crystalline slip, that is, Stage I crack growth zone, is 20~60μm and depend on stress amplitude. The size of bright facet area (granular area) in the vicinity of inclusion including the size of inclusion, $\sqrt{area_{facet}}$, was also measured. The $\sqrt{area_{facet}}$ is 40~19μm and increases as decreasing of stress amplitude.

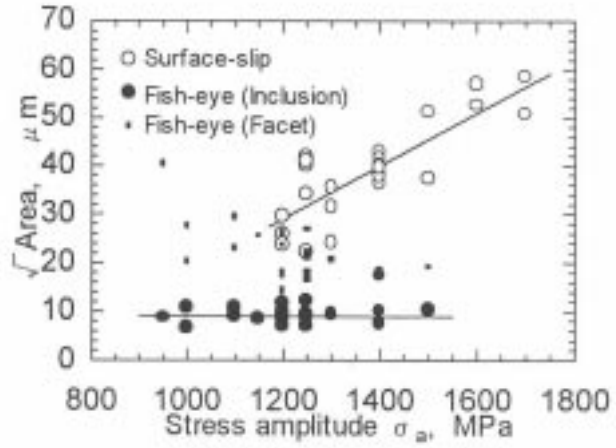

Figure 4: Experimental relationship between size of crack initiation site and stress amplitude.

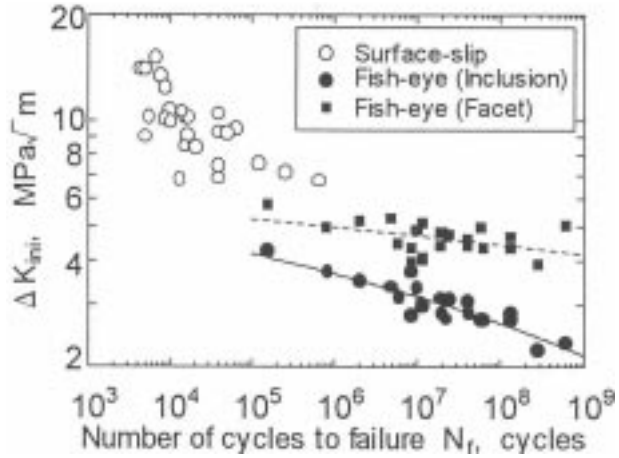

Figure 5: Experimental relationship between stress intensity factor range at crack initiation site and number of cycles to failure.

Stress Intensity factor at Crack Initiation Site

Based on the size of crack initiation site, initial stress intensity factor range, ΔK_{ini}, was calculated using the following formulas [6];

$$\Delta K_{ini,S} = 0.65\sigma_a\sqrt{\pi\sqrt{area_S}}\ , \quad \text{for surface crack initiation} \qquad (1)$$

$$\Delta K_{ini,inc} = 0.5\sigma_{at}\sqrt{\pi\sqrt{area_{inc}}}\ , \quad \text{for internal crack initiation} \qquad (2)$$

where, σ_{at} in Eqn (2) is true stress amplitude applied to the inclusion. Figure 5 shows the relationship between ΔK_{ini} and number of cycles to failure, N_f. Both of ΔK_{ini} are decreased increasing N_f. $\Delta K_{ini,S}$ for surface crack initiation distributes in 15~6 MPa√m and $\Delta K_{ini,inc}$ for

internal crack initiation is in range of 4~2 MPa√m. Therefore, it is understood that a crack occurred at inclusion can be propagated under the smaller stress intensity factor range compared with that of surface crack mode. The minimum value of 6 MPa√m for $\Delta K_{ini,S}$ is suggested as the threshold stress intensity factor range, ΔK_{th}, for surface crack growth.

Surface crack growth behavior was examined under the applied stress amplitude of 1450 and 1500 MPa using three specimens. Experimental results of crack growth rate, *da/dN* are shown in Figure 6 in relation to stress intensity factor range, ΔK, which is calculated assuming as semi-circular shaped surface crack. From this figure, it can be obtained that the ΔK_{th} for surface crack growth is 5 MPa√μ and same as the minimum value of $\Delta K_{ini,S}$. Therefore, it is suggested that the fatigue limit obtained from the staircase method is defined as the limit of surface crack initiation or growth.

Stress intensity factor range of the bright facet area in the vicinity of inclusion, $\Delta K_{ini,facet}$, was calculated using the $\sqrt{area_{facet}}$ in Figure 5 and Eqn (2). The obtained results are shown in Figure 5. It was found from the figure that the $\Delta K_{ini,facet}$ is in the range of 4~6 MPa√m and shows less dependency on N_f as compared with $\Delta K_{ini,inc}$. Because that the $\Delta K_{ini,facet}$ shows the same value as the ΔK_{th} for surface crack growth, It is expected that the internal fracture mode initiated from inclusion is governed by the formation of bright facet area in the vicinity of inclusion. Formation mechanisms does not clear at this time but it is suggested that crack growth rate is very slow in the bright facet area because of long fatigue life.

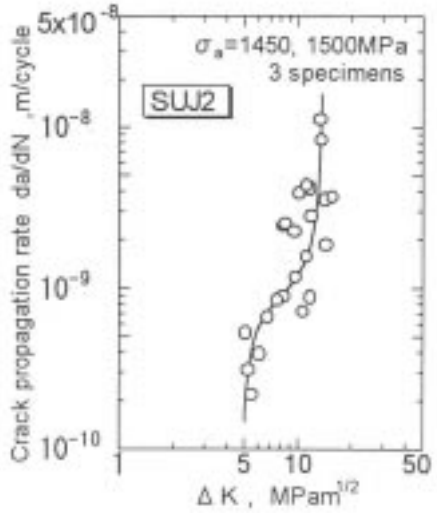

Figure 6: Surface crack growth rate relating with ΔK.

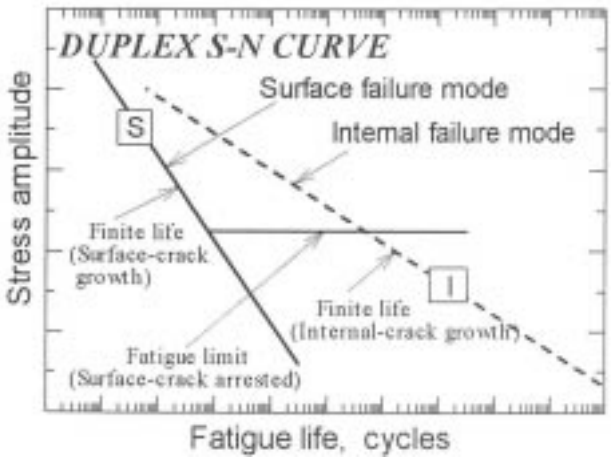

Figure 7: Schematic illustration of duplex S-N curve.

Characteristics of S-N Curve

From the experimental results obtained in this study, S-N curve of this steel shows quite different characteristics as compared with a step-wise S-N curve reported by some researchers. Both the fatigue data of surface and internal fracture mode are distributed in wide range of stress amplitude level putting between the horizontal step in the S-N curve. Therefore, it is convenient to understand the S-N characteristics that two different S-N curves corresponding to the respective fracture mode exist in this steel as shown schematically in Figure 7. From this point of view, the present type of S-N characteristics can be called as duplex S-N curve instead of step-wise S-N curve. One of two S-N curves appears at high stress amplitude revel and in low cycles of lifetime due to the surface crack initiation and growth as indicated by solid line in this figure. Fatigue fracture in the finite life range is caused by the gradual growth of microcracks initiated in slip bands on the specimen surface, because that the surface has favorable conditions for nucleation and growth of cracks compared with inside the body due to geometrical-mechanical conditions. A fatigue limit

appears at a critical stress amplitude where the initiated surface microcracks are arrested. The resistance, which is affected by microstructure, hardness and residual stress distribution in materials, will control the possibilities of surface crack initiation and propagation [5]. The common fatigue limit σ_w is estimated by the following empirical equation;

$$\sigma_w = (HV \times 9.8)/6 \qquad (3)$$

Calculated value of this steel is 1225±25MPa and good agreement with the experimental result obtained by the staircase method within the scatter of ±0.1HV.

Another S-N curve appears in high cycles of lifetime due to the internal crack initiation and growth as indicated by dashed line in Figure 7. The mechanism for the internal fatigue fracture is fundamentally the same as for the surface fatigue fracture mode. The resistance to crack initiation and propagation will control the possibility that the fatigue fracture mode is surface or subsurface. Even if crack initiation takes place simultaneously at both surface and interior, the surface fatigue fracture may be occur in advance of the internal fracture because that crack propagation at subsurface is slower than at the surface due to the difference of environmental effect between inside and outside the material. Commonly, fracture by the internal fatigue process is observed only when the surface fatigue process is suspended, that is, below the fatigue limit of the surface fracture. However, it can be clearly found from Figure 1 that the S-N curve of surface and internal fracture mode reveals doubly in wide range of applied stress amplitude. It is difficult to give the answer at this time why both fatigue fracture take place simultaneously. The answer may be obtained by the consideration of the

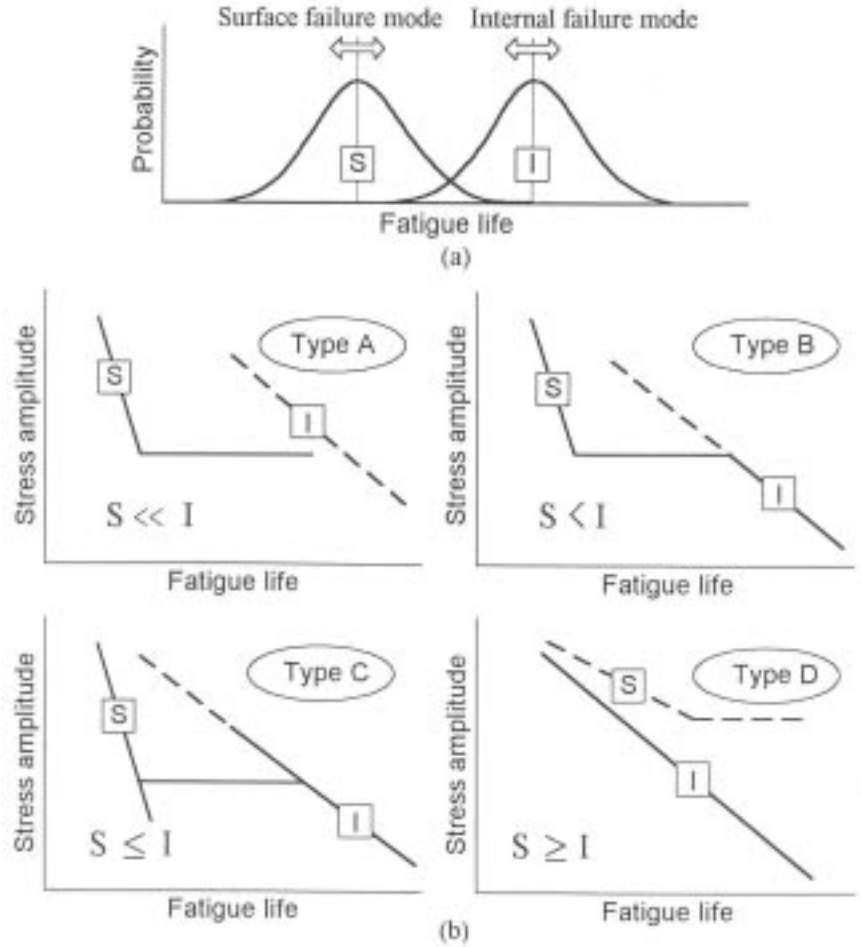

Figure 8: Classification of S-N curve using the concept of duplex S-N curve.

probability of fracture occurrence for the both modes.

Based on the concept of duplex S-N curve of materials, S-N characteristics of many steels reported in the literatures will be classified to four types of S-N curve as shown schematically in Figure 8. Each S-N curve reveals as the results corresponding to the relative position on the probability distribution of occurrence for surface and internal fatigue fracture mode of the individual material [see Fig. 8(a)]. And also this position depends on the stress amplitude level. First, Type A is common S-N curve of low-carbon steels governed by the surface fracture mode, and internal fracture mode occurs at infinite lifetime. Type B is well known as step-wise S-N curve. In this case, the probability distribution of surface fracture mode is separated from that of internal fracture mode. Type C is called as duplex S-N curve in this study. The position of probability distribution of internal fracture mode is close to that of surface fracture mode, and the both are overlapped partially. Finally, Type D is the S-N curve governed by the only internal fracture mode because the probability distribution of internal fracture is in the shorter lifetime than that of the surface fracture mode.

CONCLUSIONS

(1) The S-N curve obtained from high carbon-chromium bearing steel was clearly classified fracture modes into two groups of different crack origin. One was governed by a crystal slip on the specimen surface and the other was governed by nonmetallic inclusion at subsurface.
(2) The inclusion governed fish-eye fracture mode was distributed in a wide range of stress amplitude not only below the fatigue limit defined as the threshold of fracture due to the crystal slip governed mode but also above the fatigue limit.
(3) This remarkable shape of the S-N curve was different from a step-wise one reported in literature and was characterized as duplex S-N curve which composed of two different S-N curves corresponding to the respective fracture modes.
(4) Bright facet area was observed in the vicinity of a nonmetallic inclusion at the fracture origin inside a fish-eye mark. It was suggested that the formation of this area during long fatigue process controlled the internal fracture mode.
(5) An examination of the initial stress intensity factor range of fracture origin, ΔK_{ini}, showed that theΔK_{ini} of the slip governed fracture mode was larger than the threshold stress intensity factor range of the surface crack growth, ΔK_{th}. On the other hand, cracks originate and propagate from inclusion at subsurface with smaller ΔK_{ini} than the slip-originating crack and the ΔK_{th}.

REFERENCES

1. Wang, Q. Y., Berard, Y., Dubarre, A., Baudry, G., Rathery, S. and Bathias, C. (1999) *Fatigue Fract. Engng. Mater. Struc.*, **22**, 667-672.
2. Murakami, Y., Nomoto, T. and Ueda, T. (1999) *Fatigue Fract. Engng. Mater. Struc.*, **22**, 581-590.
3. Nishijima, S. and Kanazawa, K. (1999) *Fatigue Fract. Engng. Mater. Struc.*, **22**, 601-607.
4. Sakai, T., Takeda, M., Shiozawa, K., Ochi, Y., Nakajima, M., Nakamura, T. and Oguma, N. (1999) *Fatigue'99*, **1**, 573-578.
5. Shiozawa, K., Nishino, S., Ohtani, T. and Mizuno, S. (1999) *Small Fatigue Cracks: Mechanics, Mechanisms and Applications*, Ed. by Ravichandran, K. S., *et al*., 39-47.
6. Murakami, Y. (1993) *Metal Fatigue: Effect of Small Defects and Nonmetallic Inclusions*, Yokendo, Tokyo.